SMALL AMPLITUDE ELASTIC BUCKLING OF A BEAM
UNDER MONOTONIC AXIAL LOADING, WITH FRICTIONLESS CONTACT
AGAINST MOVABLE RIGID SURFACES

Francesco Genna and Guido Bregoli

msp

msp

SMALL AMPLITUDE ELASTIC BUCKLING OF A BEAM UNDER MONOTONIC AXIAL LOADING, WITH FRICTIONLESS CONTACT AGAINST MOVABLE RIGID SURFACES

FRANCESCO GENNA AND GUIDO BREGOLI

The elastic buckling of planar beams in the presence of frictionless unilateral contact against rigid surfaces is reconsidered, taking also into account a possible elastic translation of the rigid surfaces with respect to each other. Exclusive reference is made to the case of small amplitude deflections, such as it is expected to occur in the engineering application of buckling-restrained braces, where the gap between the brace itself and the external containment structure is normally extremely small. Even though this case precludes the occurrence of several deformed shapes possible for the general case of large displacement (to be treated like Euler's elastica), already described in the literature, a significant variety of behaviors is still possible. Only monotonic loading is considered. The main variables under investigation are (i) the wavelength of the buckled beam for a given value of the axial shortening and (ii) the total thrust exerted by the buckled beam against the rigid constraints. It is found that both variables can assume several possible values under the same load; in some cases, their values can be bounded analytically. It appears that, even in the extremely simplified case considered here, the actual behavior is dominated by the existing imperfections, both mechanical and geometrical, thus being quite difficult to be predicted with accuracy.

1. Introduction

The work herein described concerns the post-buckling analysis of a compressed elastic beam placed between two rigid surfaces, that create a frictionless unilateral constraint to the deflection amplitude. The work done so far, which seems to have started with [Villaggio 1979], approaches this problem in a general framework, i.e., for arbitrarily large displacements, in terms of Euler's equations for the so-called elastica. In few instances, such as [Chai 1998], a detailed analysis is developed also for the special case of small amplitude, i.e., exploiting a second-order theory. In the work published so far the main goal was to follow the evolution of the first waves of the deformed shape, once in contact against the external rigid surfaces; a remarkable variety of configurations was found to be possible.

In the present work, the attention is focused only on the case of small amplitudes. The motivation for this analysis is the determination of the buckled configuration of the core plate of a steel buckled-restrained brace (BRB)[1] for a given axial shortening displacement, as well as of the thrust exerted by the buckled core against the external confinement profiles. In this situation, the usually small gap left

---

[1] A steel-bolted BRB is an innovative type of brace, designed to dissipate energy, upon horizontal loading such as wind- or earthquake-induced, both in tension and in compression. It is made of a steel plate enclosed into two bolted steel struts that act as a retaining case, with an internal empty gap.

between the facing surfaces of the inner core of the BRB and the external containment guarantees for small amplitude buckling, so that an analysis developed in a second-order theory is fully adequate. At the same time, this analysis eliminates from the picture a significant portion of the complexity inherent into the elastica solutions, thus allowing some closed-form solutions.

The real case of the BRBs involves, of course, friction and plastic dissipation. Nevertheless, in order to obtain first indications about both the number of waves formed by the buckled core for a prescribed axial shortening, and about the lateral thrust, it appears useful to start the analysis from the simplest possible case, i.e., the one schematically illustrated in Figure 1: linear elastic material; frictionless unilateral contact between core and containment profiles; containment treated as a rigid surface.

The post-buckling deformed shape is here assumed to have a small amplitude, since the gap s between core and rigid constraints is always assumed to be very small. As a consequence, the average axial strain is given only by the axial deformation, with no contribution given by the post-buckling bending. This is true as long as the wavelength does not become extremely short, a circumstance that here is ruled out, limiting the interest to engineering situations for which the average axial shortening strain of the buckled core is of the order of 0.01.

In the present work, no attempt is made at dealing with cyclic loading, which seems to cause a very strange inelastic behavior, according to [Chai 1998], even in the presence of a fully conservative situation. This aspect alone deserves a separate analysis, for which there is no space here.

The rigid constraints are not assumed to be fully fixed to the reference system, and are thus unable to transmit reaction forces to it. In an attempt at describing the real arrangement of BRBs, the two rigid surfaces are connected to each other by an elastic spring, whose stiffness can range from any finite value up to infinity. In this situation, the rigid surfaces can only translate following the internal core thrusts, so that the lateral thrust at one side of the core must equal the one at the opposite side. This is an essential difference with respect to all the previous work published on this topic.

The main goal is to obtain in a direct way, given a value Δ of the axial shortening displacement, (i) the number of buckled waves, (ii) the associated axial force and (iii) the total lateral thrust. It is worth repeating that in all the previous analyses these were never the main points of interest. [Chai 1998] illustrates how to follow the evolution of the post-buckling configuration, but it does not provide an indication of how to calculate directly the quantities of engineering interest.

Other works [Domokos et al. 1997; Holmes et al. 1999; Tzaros and Mistakidis 2011; Alart and Pagano 2002; Pocheau and Roman 2004] consider essentially the elastica problem, and are focused to either mathematical or computational aspects. More work has been devoted to the case of plates [Muradova and Stavroulakis 2007; Chai 2001; 2002; Roman and Pocheau 2002], but never with an engineering-oriented viewpoint. In all cases, the interest has mainly been on following the evolution of the first few waves, a problem quite difficult in itself, but of little engineering interest, for instance in view of the inevitable — and uncontrollable — effect of the existing imperfections.

In the approach illustrated in the present work, two main methodological contributions could be pointed out, both potentially useful to give an answer to the problem of calculating directly the engineering quantities of interest.

A first one is the adoption of the total potential energy as a tool to identify, when necessary and when possible, the number of buckled waves. This technique was already adopted in [Genna and Gelfi 2012b], but in a more restricted framework.
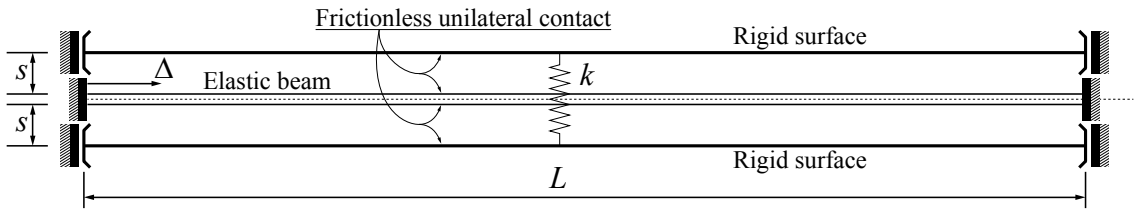
Figure 1. Geometry of the problem under consideration.

A second idea is to choose the buckled wavelength as the main unknown, instead of the number of waves as done previously (for instance, in [Chai 1998]). The number of waves is an integer number that depends on all the geometrical and material data of the problem, whereas the wavelength turns out to be governed by a parameter much easier to be computed, and independent of the total length of the beam. In the case of an infinitely rigid connection spring, such a parameter can take values in a reasonably restricted set.

Since the application envisaged here concerns the post-buckling behavior of BRBs, it is deemed important, upon examination of both numerical and experimental results [Bregoli 2014; Genna and Gelfi 2012a; 2012b; Gelfi and Metelli 2007], to take into account post-buckling shapes not previously considered in the available literature, i.e., for instance, nonsymmetric ones, with point contact at one side of the beam and line contact at the other. Even though the restriction to the small-amplitude case prevents the much wider range of shapes allowed by the elastica case, a significant potential complexity can still be shown, that requires attention.

The analysis illustrated in the sequel will consider initially the general case of an elastic spring connecting the two rigid surfaces. For the special case of a rigid connection, some closed-form results are obtained; the conflicting effects of the elasticity of the constraint will be shown.

2. Analysis of the problem

The geometry of Figure 1 is considered, which refers to rigid surfaces that can only translate according to the force generated into the connecting elastic spring by the thrust of the buckled core.

Although equilibrium is imposed on the deformed configuration, both displacements and strains are assumed to be infinitesimal (i.e., second-order approximation); shear strain contributions are neglected.

It is assumed, for simplicity, that any existing imperfection amplifies the first eigenvector of the elastic beam. Were this not the case, the initial transient phase, after first buckling of the core, might be considerably different from what described in the following, even though, eventually, some clearly defined state, among those illustrated next, should be reached anyway.

The buckled deformed shape is assumed to be periodic along the beam length. This assumption entails some difficulties. The first one concerns the initial transient stage, which is dominated by the imperfections and is hardly periodic in any real situation. When the number of waves increases, the configuration tends to be slightly less sensitive to imperfections, and to become more and more periodic, although never exactly so. If everything were perfect and periodic, each wave would buckle and form a new wave at the same time, thus causing an instantaneous multiplication of the wave number. On the contrary, as also observed in [Chai 1998], in experiments, but also in numerical simulations that
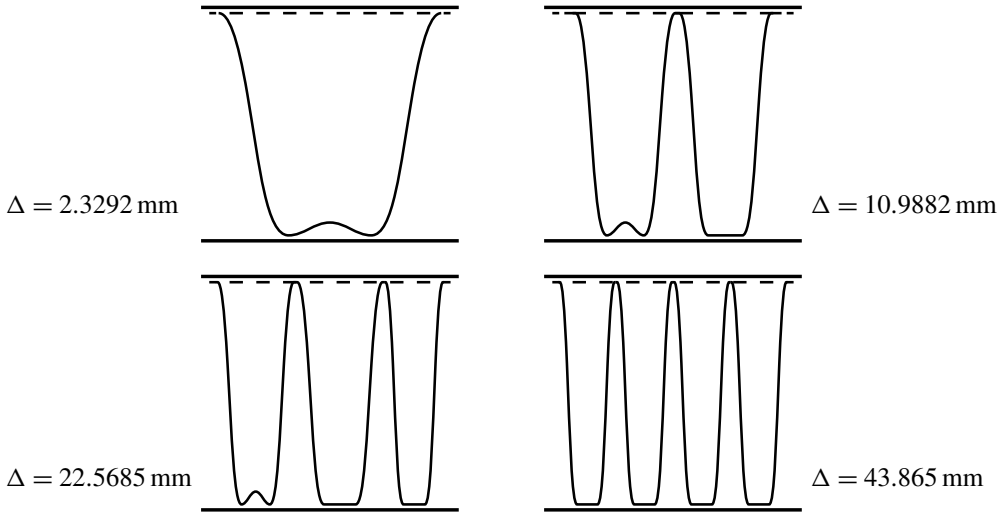
Figure 2. Deformed shape, magnified by a factor of 100, at four axial displacement
values for a beam problem adopting the data of Figure 5 of [Chai 1998]. Dashed lines
indicate undeformed shapes; thick solid lines indicate the final position of the rigid
containment surfaces. FEM solution; 500 Timoshenko linear beam elements. Data as
noted in the text.

must include some imperfection in order to exhibit buckling, the number of waves increases every time
by one, for increasing axial shortening. This effect could be once more attributed to the existence of
imperfections. The new configuration, when a new buckled wave is generated, is again (almost) periodic
anyway.

The analysis of the possible evolution of the buckled configuration may start from the observation of
a finite element (FEM) solution, shown in Figure 2. This solution is obtained by means of the commer-
cial code ABAQUS [Hibbitt et al. 2013], and refers to the case of an infinitely rigid connection spring.
The data reproduce the example analyzed in [Chai 1998], and are: length $L = 3000$ mm; rectangular
cross-section 120×10 mm; gap $s = 15$ mm; Young's modulus $E = 210000$ MPa; axial shortening
$\Delta = 43.865$ mm, so as to have a final value of Chai's parameter η equal to $\eta = 400$, as in Figure 5 of [Chai
1998]. The numerical analysis adopts a mesh of 500 Timoshenko 2-noded beam elements; it is conducted
for prescribed axial shortening, in a regime of arbitrarily large strains and displacements. An initial
geometrical imperfection is defined as an irregularity of the axis line of the beam, of the order of $\pm s/600$.

Figure 2 shows a remarkable complexity in the evolution of the buckled shape. It shows both the
point and the line contacts described in [loc. cit.], but it also shows that a very common occurrence is
a buckled shape having a line contact followed, along the axis line of the beam, by a point one. This
occurrence is also found, both experimentally and numerically, in the analysis of BRBs in the elastic-
plastic range [Genna and Gelfi 2012a], and it seems necessary to include it in the calculations concerning
the lateral thrust.

A qualitative analysis of the evolution of the post-buckled shape of this type of structure seems to lead
to the following possibilities.

2A. *Initial contact.* Before contact occurs, the situation is purely Eulerian. In the absence of imperfections a bifurcation would occur, of no practical interest. In a real case, what happens first depends strongly on the existing imperfections, that can lead to the formation of one or more than one contact points, in a way impossible to predict. As said, we will consider, for simplicity, only a case in which the first contact occurs at a single point.

Figure 3 illustrates the first stages of the post-buckled configuration. Each image shows a single wave, of length $2l_0$, of the deformed shape $v(z)$ at the top, and the corresponding bending moment $M(z)$ diagram at the bottom. Image 1, if $2l_0 = L$, refers to the time following the first contact. At the contact point, a local concentrated force (thrust) Q_i causes a local reduction of the bending moment. For increasing axial shortening, the increase of the thrust reduces the bending moment at the contact point until it becomes equal to zero (image 2). At this moment, two possibilities exist, as discussed in quantitative terms in the next section: (i, image 3a), one of the single half-waves buckles, thus forming a new wave with a new point contact situation; (ii, images 3b and 3c), the point contact becomes a line contact before any further local buckling occurs. This latter situation can be of two different types: a symmetric line contact, as in image 3c, or an asymmetric line contact, as in image 3b, with a line contact at one side and a point contact at the other. Which path will be actually followed depends on the existing imperfections; there seems to be no indication, from the theory, about a preferred path.

In order to simplify the presentation, the acronym PC will be used from now on to denote a pure point
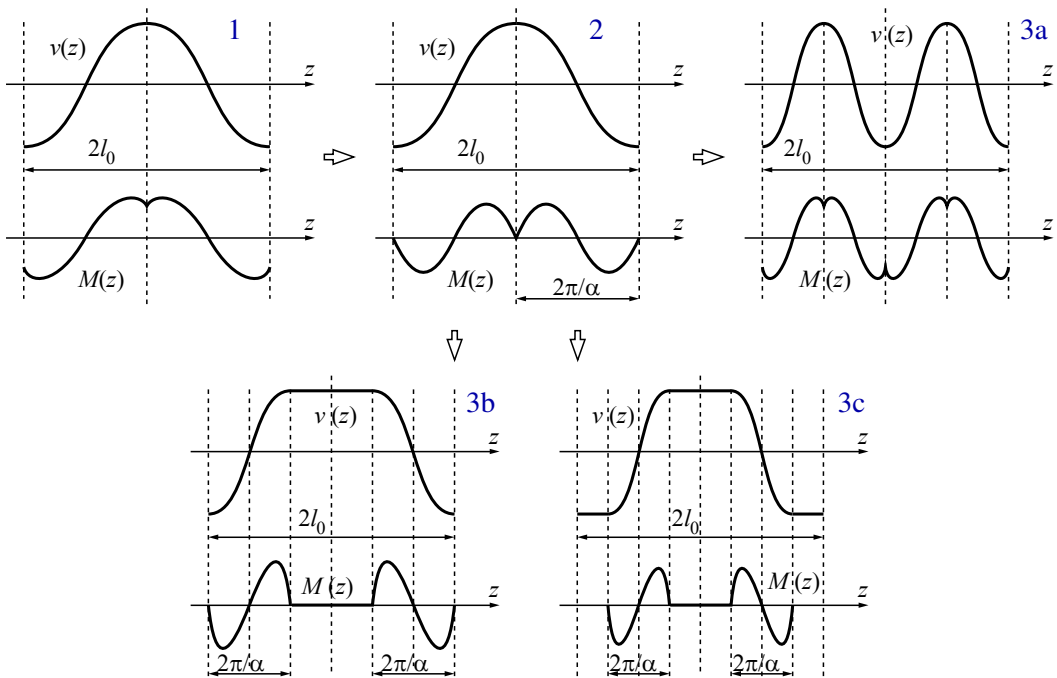
Figure 3. Possible evolution of the buckled shape after the first contact. One or two buckled waves are depicted. Image 2 refers to the instant when both the inclined portions of the beam reach a critical axial load value, with zero bending moment at the contact point. Images 3a, 3b, and 3c illustrate possible evolutions from the situation of image 2.
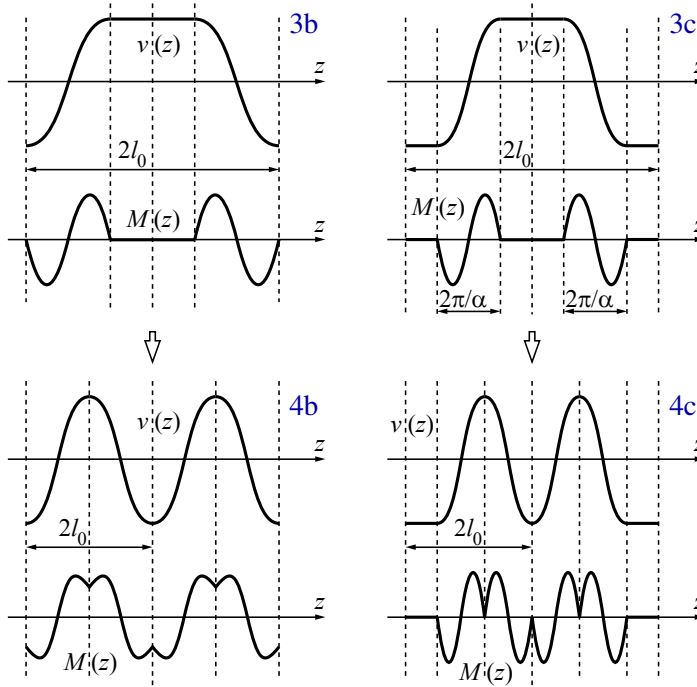
Figure 4. Possible evolution of the buckled shape from line contact situations. Images 3b and 4b refer to the evolution from an ALC configuration, and images 3c and 4c to the evolution from an SLC configuration.

contact situation; SLC will indicate a symmetric line contact, and ALC will indicate an asymmetric line contact as in image 3b of Figure 3.

2B. *Evolution from a PC situation.* Consider first a PC configuration like the one of image 1 in Figure 3, where now, in general, a single wave does not represent the full length of the beam. Recall that, despite the assumed periodicity, each time there is a local buckling only one new wave is generated, and the rest of the beam rearranges its configuration, according to the existing imperfections, in order to restore periodicity. Upon an increase of the axial shortening, any of the situations of Figure 3, images 3a, 3b, and 3c, can be reached next.

2C. *Evolution from an ALC situation.* Figure 4 shows the possible evolutions from both the line contact configurations. In the case of an ALC (images 3b and 4b), either one flat portion buckles, or one of the inclined portions buckles. In both cases, always assuming that only a single new wave can appear, and that periodicity must be restored, the next configuration has to be a PC one, illustrated in image 4b.

2D. *Evolution from an SLC situation.* Image 4c in Figure 4 shows the possible evolution from an SLC situation. In both the events that one flat portion or one inclined portion of a wave buckles, a new ALC configuration is reached.

It seems that in some cases, such as in Figure 4, image 4b, the bending moment at the point of the new contact can be nonzero independently of the number of preexisting waves. This condition would rule out
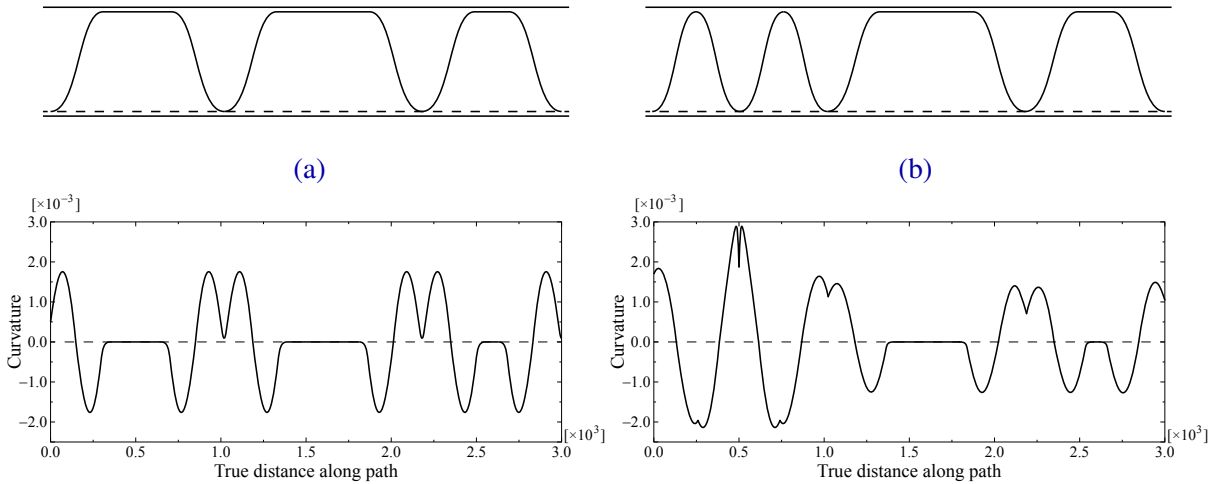
Figure 5. FEM analysis of the problem of Figure 2. Deformed shape (top, magnified by a factor of 20) and elastic curvature (bottom) at two successive times (a) and (b) during the post-buckling history. A line contact — the one at the extreme left in (a) — , with zero bending moment along it, transforms into a point contact with nonzero bending moment at the contact point, seen in (b). Dashed lines indicate undeformed shapes; thick solid lines indicate the final position of the rigid containment surfaces.

the possibility that the formation of a new wave occurs directly with a new line contact configuration: a line contact configuration, in fact, has zero bending moment all along the flattened portion of the beam. This can also be shown numerically: Figure 5 illustrates two successive instants during the deformation history of the same beam of Figure 2. At the first instant, on the left, a sequence of ALC configurations appears. At the second instant, on the right, after a little increment of the prescribed axial displacement, the left flat portion of the beam has buckled, forming a new wave with a new point contact situation. The bending moment, at the new contact point, is nonzero, as shown in the corresponding bottom image.

Several numerical solutions of this problem, with different geometries and different gaps, have always shown the evolution from one situation to another in terms of what described above. As apparent even from Figure 2, in a "real" case a full periodicity is not always reached, and, moving along the beam axis, one might encounter a sequence of PC, SLC, and ALC waves. Nevertheless, in order to perform analytical calculations to estimate the parameters of interest, full periodicity must be assumed anyway, as done in the next section.

3. Analytical calculation of the wavelength and associated lateral thrust

The technique adopted in this section is in part similar to that proposed in [Chai 1998], but has several important differences:

- Contact may occur, in general, against rigid surfaces that can translate, being connected to each other by an elastic spring. This could be either a distributed elastic foundation or, fully equivalently,

a single elastic spring as shown in Figure 1. The spring constant k of Figure 1 is in fact equivalent to the value of a foundation constant per unit length multiplied by the total length L of the beam.

- All the possibilities illustrated in the previous section are considered.

- The analysis considers as a main unknown the buckled wavelength, independent of the total length of the beam.

- The analysis aims at determining directly the wavelength corresponding to a given axial shortening.

- The beam total axial shortening Δ derives, in general terms, from both the axial deformability and the post-buckling bending, i.e., in a second-order theory,

$$\Delta = \bar{\varepsilon} L + \int_0^L \tfrac{1}{2}(v'(z))^2 \, dz, \tag{3-1}$$

where $\bar{\varepsilon}$ indicates the average membrane strain due to the axial stiffness, assumed positive if associated to shortening. In the sequel of this work, shortening and compression will always be assumed as positive.

Nevertheless, the assumption of a small value for the gap s, and the consequent adoption of a second-order theory, make it appropriate to neglect the bending contribution when considering the boundary conditions of the problem. This is true as long as the number of buckled waves does not become excessively high, a situation that can be easily ruled out in engineering applications. Therefore, in the sequel of this work the following global boundary condition will be adopted:

$$\Delta = \bar{\varepsilon} L. \tag{3-2}$$

In real applications, such as BRBs, the prescribed value of Δ can derive from any type of horizontal loading, such as wind or earthquake-induced, acting on a frame which includes the considered structural element as a bracing structure. The frame stiffness is usually much greater than the BRB stiffness; therefore, the ends of the BRB can be considered as hinged (or fully fixed, depending on the connection design), and subjected to a prescribed displacement.

3A. *Equations for the case of point contact.* Figure 6 shows the considered geometry and the adopted reference systems for the most general case of a point contact situation (solid lines only). The Figure shows a generic half-wave, of length l_0, of the beam deformed shape. In this configuration, the two beam portions at the extreme left and right sides correspond to originally flat portions that have buckled simultaneously, forming each a new wave, possibly of different length at each side. Although such a situation has been ruled out a priori, previously, one can start from it from the sake of generality, and analyze its implications.

In all the calculations developed in the following, the buckled shape is assumed to be periodic along the beam length.

The two central inclined portions of the beam must have equal length, defined by the unknown parameter β, $0 < \beta \leq \tfrac{1}{2}$, in order to satisfy the geometric boundary conditions and in order to have the same force at the points of contact with the rigid surfaces (this could be checked analytically). This is an important consequence of the arrangement of Figure 1, which has no constraint for the absolute vertical
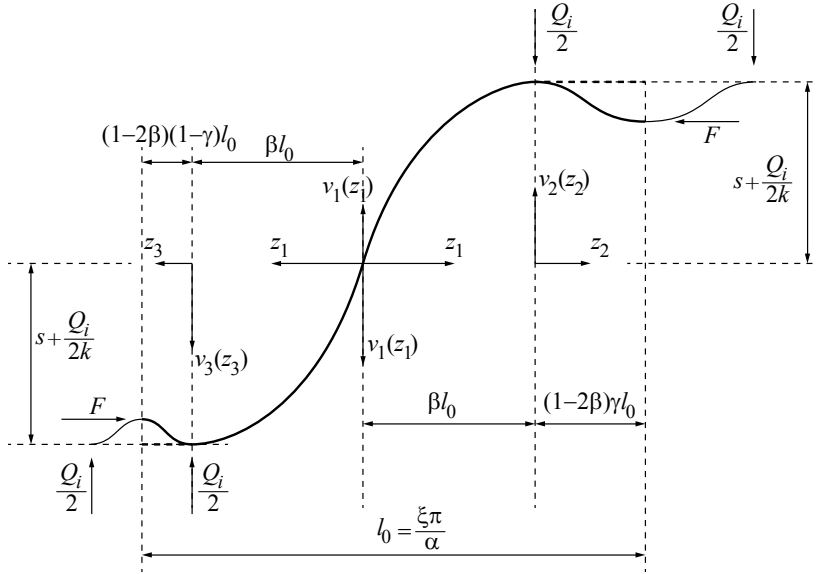
Figure 6. Structural scheme of a single half-wave of the buckled deformed shape. The solid lines represent a generic configuration of point contact. The dashed lines represent a generic configuration of line contact. Parameters ξ, β, and γ are unknown and define the geometrical properties of the half-wavelength l_0.

translations of the rigid surfaces, in such a way that the total contact force acting on one surface must be equal to the corresponding force acting on the other.

The two lateral portions of the beam are initially assumed to have a different length, defined by the unknown parameter γ, $0 \le \gamma \le 1$.

As a consequence of this arrangement, only three different reference systems must be adopted for a single half-wave: one, indicated by z_1, refers to the two central portions of the beam, whose deflection is denoted by $v_1(z_1)$; the two lateral portions of the beam are referred to systems z_2 and z_3, respectively, and their deflections are denoted by $v_2(z_2)$ and $v_3(z_3)$, for the right and the left portions, respectively, with the conventions of Figure 6. Correspondingly, the bending moment for $z_1 = 0$, a point of flex for the deformed shape, is zero.

The axial force corresponding to the prescribed displacement Δ is denoted by F; owing to the assumption of small displacements and linear elasticity, the following relation holds:

$$F = EA\bar{\varepsilon} = \frac{EA}{L}\Delta, \tag{3-3}$$

where E denotes the Young's modulus of the beam, and A the beam's cross-sectional area.

At each contact point, the corresponding contact force is denoted by $Q_i/2$, Q_i indicating the unit thrust, i.e., the thrust associated to a single wave at each side of the buckled beam. The total thrust at each side of the beam, i.e., the force acting inside the connection spring, is given by

$$Q = Q_i N, \tag{3-4}$$

where N denotes the total number of buckled waves. Here, and for a while next, the following relationship is adopted, to relate the number of waves N to the half-wavelength l_0:

$$N = \frac{L}{2l_0}. \tag{3-5}$$

Finally, the maximum amplitude of the buckled shape, at all the contact points, is given by

$$v_1(\beta l_0) = v_2(0) = v_3(0) = s + \frac{Q}{2k}. \tag{3-6}$$

This condition follows from the infinite bending stiffness of the external surfaces; one must also recall that the total elongation of the connection spring between the rigid surfaces, equal to Q/k, is twice the difference between the maximum amplitude $v_1(\beta l_0)$, at each side of the buckled beam, and the gap s.

It is possible, on the basis of the scheme of Figure 6, to write both the bending moment equations in all the beam parts, and the differential equations governing the deformed shapes:

$$M_1(z_1) = F v_1(z_1) - \tfrac{1}{2} Q_i z_1, \quad 0 \le z_1 \le \beta l_0,$$
$$M_2(z_2) = F v_2(z_2) - \tfrac{1}{2} Q_i \beta l_0, \quad 0 \le z_2 \le l_0(1 - 2\beta)\gamma,$$
$$M_3(z_3) = F v_3(z_3) - \tfrac{1}{2} Q_i \beta l_0, \quad 0 \le z_3 \le l_0(1 - 2\beta)(1 - \gamma), \tag{3-7}$$

$$EI v_1''(z_1) = - M_1(z_1), \quad EI v_2''(z_2) = -M_2(z_2), \quad EI v_3''(z_3) = -M_3(z_3), \tag{3-8}$$

where the bending moments are assumed positive if causing tension in the top fibers in the two right portions of the beam, and in the bottom fibers in the two left portions of the beam, and I indicates the relevant moment of inertia of the beam cross-section: here, this will always assumed to be the minimum principal moment of inertia. Inserting (3-7) into (3-8) and rearranging terms in the usual way, one obtains:

$$v_1''(z_1) + \alpha^2 v_1(z_1) = \frac{Q_i \alpha^2 z_1}{2F}, \quad v_2''(z_2) + \alpha^2 v_2(z_2) = \frac{Q_i \alpha^2 \beta l_0}{2F},$$
$$v_3''(z_3) + \alpha^2 v_3(z_3) = \frac{Q_i \alpha^2 \beta l_0}{2F}, \tag{3-9}$$

where

$$\alpha^2 = \frac{F}{EI}. \tag{3-10}$$

The half-wavelength l_0 is redefined in terms of the following nondimensional parameter ξ, which, together with parameters β and γ introduced earlier, will be the main unknown of this problem:

$$l_0 = \xi \frac{\pi}{\alpha} \tag{3-11}$$

in such a way that the following also holds:

$$F = \xi^2 \frac{\pi^2 EI}{l_0^2}. \tag{3-12}$$

This allows an immediate comparison of the results for the wavelength with the standard Euler results for elastic buckling, where $\xi = 1$ always.

The relevant boundary conditions are as follows:

$$v_1(0) = 0, \tag{3-13}$$

$$v_1(\beta l_0) = v_2(0) = v_3(0) = s + \frac{Q}{2k}, \tag{3-14}$$

$$v_1'(\beta l_0) = 0, \tag{3-15}$$

$$v_2'(0) = v_3'(0) = 0, \tag{3-16}$$

$$v_2'[l_0(1 - 2\beta)\gamma] = 0, \tag{3-17}$$

$$v_3'[l_0(1 - 2\beta)(1 - \gamma)] = 0. \tag{3-18}$$

The integration of equations (3-9) yields the following results:

$$v_1(z_1) = C_1 \cos \alpha z_1 + C_2 \sin \alpha z_1 + \frac{Q l_0 z_1}{FL}, \tag{3-19}$$

$$v_2(z_2) = C_3 \cos \alpha z_2 + C_4 \sin \alpha z_2 + \frac{Q \beta l_0^2}{FL}, \tag{3-20}$$

$$v_3(z_3) = C_5 \cos \alpha z_3 + C_6 \sin \alpha z_3 + \frac{Q \beta l_0^2}{FL}. \tag{3-21}$$

It is convenient to start with the analysis of functions v_2 and v_3 in (3-20) and (3-21). The equations (3-16) yield immediately $C_4 = C_6 = 0$. The equations (3-17) and (3-18) are then rewritten as:

$$-\alpha C_3 \sin [\alpha l_0(1 - 2\beta)\gamma] = 0 \quad \text{and} \quad -\alpha C_5 \sin [\alpha l_0(1 - 2\beta)(1 - \gamma)] = 0, \tag{3-22}$$

respectively. These can be satisfied in the following ways:

(1) By setting $C_3 = C_5 = 0$, which would correspond to line contact solutions, for the moment of no interest; or

(2) By prescribing what follows:

$$\alpha l_0(1 - 2\beta)\gamma = \pi, \tag{3-23}$$

$$\alpha l_0(1 - 2\beta)(1 - \gamma) = \pi, \tag{3-24}$$

which, making use of (3-11), gives

$$\gamma = \frac{1}{\xi(1 - 2\beta)} \quad \text{and} \quad 1 - \gamma = \frac{1}{\xi(1 - 2\beta)}. \tag{3-25}$$

These conditions imply

$$\gamma = \frac{1}{2}, \quad \beta = \frac{1}{2} - \frac{1}{\xi}, \tag{3-26}$$

which corresponds to a situation in which, starting from a pure SLC case, both the flat portions of the wave have just buckled, and there are two new contact points at each side of each wave.

This case, in the framework herein considered, has been ruled out, since only the formation of a single new wave at a time is allowed; nevertheless, it can, and will, be easily incorporated into the next calculations, so as to take into account also the result for ξ associated to it.

In addition to these cases, two more possibilities can be obtained from the above equations, by setting equal to zero either one or both the lengths of the lateral extremities of the wave.

The first additional case corresponds to setting, equivalently, $\gamma = 0$ or $\gamma = 1$. Let's consider only the latter choice; then, only functions $v_1(z_1)$ and $v_2(z_2)$ survive, and only the boundary condition (3-23) must be considered, which yields

$$\gamma = 1 \implies \beta = \frac{1}{2}\left(1 - \frac{1}{\xi}\right). \tag{3-27}$$

This corresponds to a situation in which, starting from a pure ALC case, the flat portion of the wave has just buckled. There is one contact point at one side of the wave, and two contact points at the opposite side.

A second additional possibility derives from setting $\gamma = 0$ and $\beta = \frac{1}{2}$, which describes a pure PC situation, in which only function $v_1(z_1)$ survives and there is only one contact point at each side of a single wave.

In this way, it is seen that the case of point contact has three possible subcases, of which one, defined by (3-26), has only a purely theoretical interest since, in practice, the existence of imperfections makes it impossible to occur.

The determination of parameter ξ for the three possible subcases follows.

For all of them, function $v_1(z_1)$ is uniquely defined by the same conditions. Prescribing the boundary conditions (3-13), (3-14), and (3-15) one obtains

$$v_1(z_1) = \frac{2\pi\xi ks[\sin(\alpha z_1) - \alpha z_1\cos(\pi\xi\beta)]}{\cos(\pi\xi\beta)(\alpha^2 FL - 2\pi^2\xi^2\beta k) + 2\pi\xi k\sin(\pi\xi\beta)}, \tag{3-28}$$

$$Q_i = \frac{4\pi\xi\alpha kFs\cos(\pi\xi\beta)}{\cos(\pi\xi\beta)(2\pi^2\xi^2\beta k - \alpha^2 FL) - 2\pi\xi k\sin(\pi\xi\beta)}. \tag{3-29}$$

Correspondingly, the bending moment associated to the function $v_1(z_1)$ is given by:

$$M_1(z_1) = EI\frac{2\pi\xi\alpha^2 ks\sin(\alpha z_1)}{\cos(\pi\xi\beta)(\alpha^2 FL - 2\pi^2\xi^2\beta k) + 2\pi\xi k\sin(\pi\xi\beta)}. \tag{3-30}$$

In all these expressions, the wavelength parameters ξ and β are still to be computed.

As proposed in [Genna and Gelfi 2012b], the parameter ξ is computed by prescribing the stationarity of the total potential energy (TPE) with respect to it. Unless one is ready to follow the complete history of the prescribed axial displacement, in fact, there seems to be no other way to determine the correct configuration associated to a given value of Δ. Even following the actual loading history, it seems difficult, in the absence of specific information about the existing imperfections, to prescribe a priori, as done in [Chai 1998], the number of waves generated by a local buckling, starting from any given configuration. Therefore, it appears that the minimization of the total potential energy is the safest tool to obtain the correct response.

In order to write the TPE, for the problem under examination, it is convenient to reconsider it as force-driven, and to express the force, at the end of the calculations, as a function of the prescribed axial shortening by means of (3-3).

The TPE for an axially compressed beam of length L, whose transversal deflection is indicated by $v(z)$ and axial displacement by $u(z)$, can be written, in a second-order theory, as follows:

$$\text{TPE}[v(z), u(z)] = \frac{1}{2} \int_0^L \left(EI(v'')^2(z) + EA(u')^2(z) \right) dz - F\Delta. \qquad (3\text{-}31)$$

In this equation, the boundary condition (3-1) should be considered for the axial shortening Δ. If one wants to distinguish between the bending and the axial contribution to the beam shortening, then the average membrane strain $\bar{\varepsilon}$ is an unknown, that can be calculated once the $u(z)$ function is obtained.

It must now be recalled that the stationarity of the TPE of equation (3-31), in a second-order theory, would furnish a bending result $v(z)$ fully uncoupled from the axial one $u(z)$.

As a consequence, exploiting the smallness of the gap s, and in order to avoid the useless complication of calculating also the unknown function $u(z)$ and the associate average strain $\bar{\varepsilon}$, here, as said, the average axial strain is assumed as known, given by (3-2), and the axial contribution to the TPE is completely ignored. Some comments about this simplification will be given in Section 4. Therefore, for the problem under investigation, the total potential energy TPE can be written, for the general configuration of Figure 6, as follows:

$$\text{TPE}[\xi] = 4N\frac{1}{2} \int_0^{\beta l_0} \left(EI(v_1'')^2(z_1) - F(v_1')^2(z_1) \right) dz_1 + 2N\frac{1}{2} \int_0^{l_0(1-2\beta)\gamma} \left(EI(v_2'')^2(z_2) - F(v_2')^2(z_2) \right) dz_2$$

$$+ 2N\frac{1}{2} \int_0^{l_0(1-2\beta)(1-\gamma)} \left(EI(v_3'')^2(z_3) - F(v_3')^2(z_3) \right) dz_3 + \frac{1}{2} 4k(v_1(\beta l_0) - s)^2 H[(v_1(\beta l_0) - s)], \quad (3\text{-}32)$$

where $H[\cdot]$ indicates the Heaviside function, required here to prescribe the existence of a contact force only if the maximum deflection of the core equals or exceeds the nominal gap s.

By prescribing the stationarity of the TPE of equation (3-32) with respect to ξ, for any choice of β and γ among the three listed above, one obtains a nonlinear equation in ξ, that, in general, must be solved numerically.

3A1. *Pure PC case, single contact point at each side.* This is the case already considered in [Genna and Gelfi 2012b], where, though, only fully fixed rigid surfaces were introduced. This corresponds to setting $\beta = \frac{1}{2}$ in the previous equations, in such a way that both functions $v_2(z_2)$ and $v_3(z_3)$, which do not exist, disappear from (3-32).

The numerical results will be presented in the next section. Nevertheless, it is of interest to furnish immediately the result in the limit $k \to \infty$. In such a case, the stationarity equation reduces to

$$\tan(\xi\pi) = \xi\pi, \qquad (3\text{-}33)$$

which has the solution

$$\xi \approx 1.4303, \qquad (3\text{-}34)$$

i.e., the result found in [loc. cit.]. In the limit $k \to \infty$, equation (3-29) for the unit thrust reduces to

$$Q_{i,\infty} = \frac{2\alpha F s \cos(\pi\xi\beta)}{\pi\xi\beta \cos(\pi\xi\beta) - \sin(\pi\xi\beta)}, \qquad (3\text{-}35)$$

which holds for all the values of β and ξ deriving from a situation of pure contact at both sides of the beam.

3A2. *Symmetric case, double contact point at each side.* In this case (3-26) holds. Adopting these values, one can obtain both the integration constants C_3 and C_5 from the boundary conditions (3-14). The result is:

$$C_3 = C_5 = \frac{2\pi\xi k s \sin\left(\frac{\pi\xi}{2}\right)}{\cos\left(\frac{\pi\xi}{2}\right)\left(\alpha^2 FL - \pi^2(\xi-2)\xi k\right) + 2\pi\xi k \sin\left(\frac{\pi\xi}{2}\right)}. \tag{3-36}$$

Accordingly, the two remaining equations for the buckled shape are:

$$v_2(z_2) = v_3(z_3) = \frac{\pi\xi k s \left(\pi(\xi-2)\cos\left(\frac{\pi\xi}{2}\right) - 2\sin\left(\frac{\pi\xi}{2}\right)\cos(\alpha z_{2(3)})\right)}{\cos\left(\frac{\pi\xi}{2}\right)\left(\pi^2(\xi-2)\xi k - \alpha^2 FL\right) - 2\pi\xi k \sin\left(\frac{\pi\xi}{2}\right)}, \tag{3-37}$$

and the TPE of equation (3-32) can be computed as a function of ξ.

As before, it is of interest to furnish immediately the result for ξ in the limit $k \to \infty$. In such a case, the equation expressing the stationarity of the TPE of equation (3-32) reduces to

$$\pi(\xi-1)\cos(\xi\pi) = \pi + \sin(\xi\pi), \tag{3-38}$$

which has the solution

$$\xi \approx 3.58639. \tag{3-39}$$

3A3. *Asymmetric case, double contact point at the top side, single contact point at the bottom side.* In this case (3-27) holds, with $\gamma = 1$. Adopting these values, function $v_3(z_3)$ disappears from the picture, and one obtains the integration constant C_3 from the relevant boundary condition of (3-14). The result is:

$$C_3 = \frac{2\pi\xi k s \cos\left(\frac{\pi\xi}{2}\right)}{2\pi\xi k \cos\left(\frac{\pi\xi}{2}\right) - \sin\left(\frac{\pi\xi}{2}\right)\left(\alpha^2 FL - \pi^2(\xi-1)\xi k\right)}. \tag{3-40}$$

Accordingly, the remaining equation for the buckled shape is:

$$v_2(z_2) = \frac{\pi\xi k s \left(2\cos\left(\frac{\pi\xi}{2}\right)\cos(\alpha z_2) + \pi(\xi-1)\sin\left(\frac{\pi\xi}{2}\right)\right)}{2\pi\xi k \cos\left(\frac{\pi\xi}{2}\right) - \sin\left(\frac{\pi\xi}{2}\right)\left(\alpha^2 FL - \pi^2(\xi-1)\xi k\right)}. \tag{3-41}$$

Once more, it is of interest to furnish immediately the corresponding result in the limit $k \to \infty$. In such a case, the equation expressing the stationarity of the TPE of equation (3-32) reduces to

$$\pi(1-2\xi)\cos(\xi\pi) = \pi - 2\sin(\xi\pi), \tag{3-42}$$

which has the solution

$$\xi \approx 2.52875. \tag{3-43}$$

3B. *Equations for the case of line contact.* A line contact starts occurring at the instant when the bending moment, at the extremities of an inclined portion of the buckled wave, becomes equal to zero. The first occurrence of this situation is illustrated in Figure 3, image 2. Upon an increase of the axial shortening, after a PC situation, the unit thrust Q_i increases until the bending moment, at the contact point, becomes zero. Thereafter, three possibilities exist, as discussed in Section 2B. A first one implies the return to a pure PC situation, with a complete rearrangement of the waves; two others imply the progressive flattening of a portion of the beam included between the points of application of half the unit thrust, as shown in images 3b and 3c of Figure 3.

In all the cases when the bending moment is zero at the extremities of an inclined portion of the beam, it is immediate to obtain the corresponding length of the inclined portion itself from (3-30), by prescribing the following condition:

$$M_1(z_1 = \beta l_0) = 0 \implies \sin(\alpha \beta l_0) = 0. \tag{3-44}$$

This implies (recall also (3-11)):

$$\beta l_0 = \frac{\pi}{\alpha} \implies \beta = \frac{1}{\xi}. \tag{3-45}$$

For the specific situation of Figure 3, image 2, i.e., the limiting case of a pure PC situation, with $\beta = \frac{1}{2}$, one thus gets

$$\xi_{\max} = 2. \tag{3-46}$$

This is the result always adopted in [Genna and Gelfi 2012b] to relate the buckled wavelength to a prescribed value of axial shortening, since the value $\xi = 2$ gave a better prediction than the theoretical result of (3-34). Genna and Gelfi [2012b], however, took into account only a PC configuration, whereas, in the previous paragraphs of the present work, it was already shown that, upon considering more general cases, even larger values for the coefficient ξ can be found.

In all the configurations of Figure 3 with zero bending moment at the extremities of the inclined parts of the wave, under the validity of (3-45), both these inclined parts have reached a local buckling load. What happens for an increase of axial shortening is not uniquely defined: as observed in Section 2, either the inclined portions buckle, or the line contact portion buckles, or, if a line contact portion does not exist yet, when $\xi = 2$ for a PC situation, flattening starts developing at the contact point. In this latter case, the unit thrust Q_i splits into separate forces of intensity $Q_i/2$ each, acting at the lateral extremities of the line contact zone. What really happens depends on the existing imperfections.

If a line contact has already developed, such as in Figure 3, images 3b and 3c, condition (3-45) allows one to easily compute all the limit situations that can derive from a line contact in the case that the next critical phenomenon is the local buckling of the flat portion. One can consider the most general situation of a line contact, which includes, as special cases, both the ALC and SLC situations considered so far. This is the configuration depicted by the dashed lines in Figure 6, where the lengths of the two flat portions can be in any ratio between each other.

The maximum value that can be reached by the wavelength parameter ξ, starting from the configuration described by the central portion of the beam plus the lateral dashed lines in Figure 6, corresponds to the first local buckling of the flat portions. Assume, with no loss of generality, that $\gamma \geq \frac{1}{2}$, so that the right flat portion of the beam buckles first. In this case, according to (3-45) and recalling definition (3-11), one has

$$(1 - 2\beta)\gamma l_0 = \left(1 - \frac{2}{\xi}\right)\gamma \frac{\xi \pi}{\alpha} = l_1. \tag{3-47}$$

The maximum value for the corresponding wavelength is obtained under the following value of the critical axial load F^*:

$$F^* = \frac{\pi^2 EI}{l_1^2}. \tag{3-48}$$

This condition, using (3-47), implies

$$\xi_{\max} = \frac{1 + 2\gamma}{\gamma}. \tag{3-49}$$

If one now recalls that the only possible values for $\gamma \geq \frac{1}{2}$ are $\gamma = \frac{1}{2}$ or $\gamma = 1$, one obtains immediately:

- For $\gamma = \frac{1}{2}$, i.e., starting from an SLC configuration:

$$\xi_{\max} = 4. \tag{3-50}$$

Note that, immediately after this situation, in principle both the flat portions of the wave would buckle, thus creating a new situation for which result (3-39) holds: the wavelength decreases in a discontinuous way.

- For $\gamma = 1$, i.e., starting from an ALC configuration:

$$\xi_{\max} = 3. \tag{3-51}$$

Note that, immediately after this situation, the flat portion of the wave buckles, thus creating a new situation for which result (3-43) holds: the wavelength decreases in a discontinuous way.

If the bending moment for $z_1 = \beta l_0$ vanishes, the unit thrust Q_i can be obtained directly from the global equilibrium of the central inclined portion of the beam, i.e., (see Figure 6):

$$F\left(s + \frac{Q}{2k}\right) = \frac{Q_i}{2}\beta l_0 \implies F\left(s + \frac{Q_i L\alpha}{4k\pi\xi}\right) = \frac{Q_i}{2}\frac{\pi}{\alpha}, \tag{3-52}$$

and has the following final expression:

$$Q_{i,M_1(\beta l_0)=0} = \frac{4\pi\xi\alpha k F s}{2\pi^2\xi k - \alpha^2 F L}, \tag{3-53}$$

which, in the limit $k \to \infty$, yields the following trivial result, independent of both ξ and L (see also [Genna and Gelfi 2012b]):

$$Q_{i,M_1(\beta l_0)=0,\infty} = \frac{2F\alpha s}{\pi}. \tag{3-54}$$

Equation (3-53) is also a particularization of (3-29) for the case in which equations (3-45) and (3-47) hold.

4. Numerical results and discussion

It was shown that the wavelength associated to a given axial shortening can be governed, according to the different possible situations, by several different values of parameter ξ. Even in the case of a rigid connection spring, the coefficient ξ takes values in the range $1.4303 \leq \xi \leq 4$. In the case of a deformable connection spring, the situation becomes definitely more complex.

In the presence of a line contact, either fully developed or incipient, the results of equations (3-46), (3-50), and (3-51), for the maximum value of ξ before a change of configuration under the condition of (3-45), hold for any value of the spring stiffness k.

On the contrary, in all the possible cases of point contact both the parameter ξ and the thrust Q depend on the stiffness of the connection spring in a complex way, illustrated, for the pure PC case (i.e., $\beta = \frac{1}{2}$), in Figures 7, 8, and 9. These figures plot, as a function of the spring stiffness k normalized by $\alpha^2 F L$, the corresponding values for ξ, Q_i, and Q, respectively. In Figures 8 and 9 the values of the thrusts have been normalized to obtain dimensionless quantities. The values for ξ have been calculated numerically, solving the stationarity equation of the TPE of equation (3-32) by means of Newton's method.
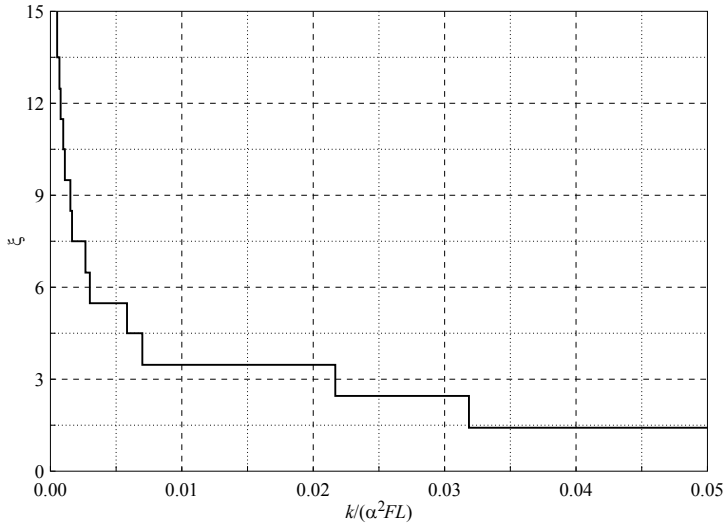
Figure 7. Values for the parameter ξ as a function of the connection spring stiffness k normalized by $\alpha^2 FL$, as computed from the stationarity of the TPE of equation (3-32) for the case $\beta = \frac{1}{2}$.
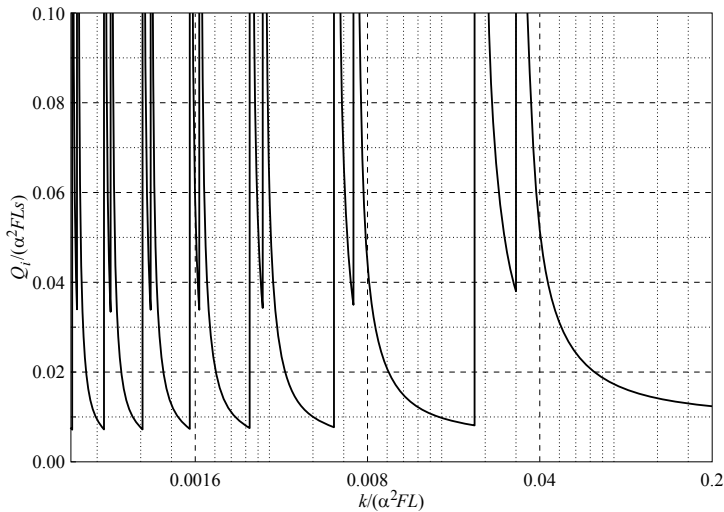
Figure 8. Values of the unit thrust Q_i, normalized by $\alpha^2 FLs$, as a function of the normalized spring stiffness $k/\alpha^2 FL$, for $\beta = \frac{1}{2}$ and ξ as in Figure 7, as given by (3-29). Other data are: rectangular cross-section 5×50 mm, $E = 210000$ MPa, $L = 560$ mm, $s = 0.5$ mm, $\Delta = 11.2$ mm.

Similar results could be shown (they are not for the sake of brevity) for different cases of point contact, i.e., for the other possible choices of the parameters β and γ as computed in Section 3A1.

The jumps of the values for ξ correspond to infinite values of the unit thrust Q_i. As can be seen from the denominator of (3-29), the normalization of k by $\alpha^2 FL$ yields values for ξ that do not depend on any further parameter.
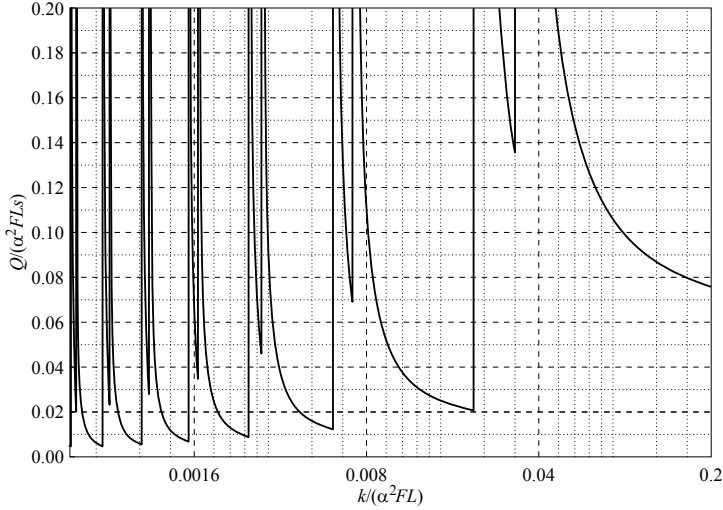
Figure 9. Values of the total thrust Q, normalized by $\alpha^2 FLs$, as a function of the normalized spring stiffness $k/\alpha^2 FL$, for $\beta = \frac{1}{2}$ and ξ as in Figure 7, as given by (3-4) and (3-5). Other data as in Figure 8.

The values for ξ take a descending step shape, staying constant in a range of values for k and then jumping to a smaller value for an infinitesimal increase of k, until the limiting value $\xi \approx 1.4303$ is reached. The jumps in the values of ξ are not of constant value, although they are all quite close to unity. In the considered range of values for k, ξ goes from $\xi \approx 15.49$ to $\xi \approx 1.4303$, which is its minimum possible value. As said, here ξ depends only on the normalized value of k, and is independent of L. This fact makes its determination simpler than the determination of the wave number N, as done in [Chai 1998] (there only for $k \to \infty$).

All the results tend to their corresponding counterparts in the limit $k \to \infty$. For finite values of k, one sees an interplay between the tendency to form less and less waves as the spring stiffness decreases (in the limit $k \to 0$ only one wave would be formed), which would imply smaller and smaller lateral thrusts, and to produce a higher thrust as the maximum displacement of the buckled shape increases, i.e., as k decreases with a constant number of waves.

The unit thrust of Figure 8 increases rapidly with decreasing k, for constant values of ξ, tending to an infinite value. The total thrust of Figure 9 follows a similar trend, in which, in addition, the tendency towards smaller values as k decreases, but for an increasing number of waves, is more apparent.

All the values of the thrust depend on all the parameters of the problem; even the value for Q_i in the limit $k \to \infty$, given by (3-54), depends linearly on the gap s and on the product αF. In addition, all the values for Q depend also on the total length L.

It is worth commenting about the effect of replacing the boundary condition in (3-2) with the boundary condition (3-1). These comments will be restricted, for the sake of simplicity, to the case of infinite stiffness of the connection spring, and only to the situation of a PC contact.

If one treats the membrane strain $\bar{\varepsilon}$ of equations (3-2) and (3-1) as an unknown, given a value of the prescribed shortening displacement Δ, then, still following the path described in the previous section, the axial force corresponding to Δ is unknown, defined by the first relationship in (3-3), and the total

potential energy of (3-31) becomes a function of the two unknowns ξ and $\bar{\varepsilon}$. In order to compute both unknowns, the easiest way is to impose (3-1) in strong form, and couple it with the stationarity of the TPE of (3-32) with respect to ξ. One thus obtains in any case the result $\xi \approx 1.4303$, and values for $\bar{\varepsilon}$ that depend essentially on the value of the gap s. For small gaps, the membrane strain tends to coincide with the nominal strain Δ/L; only for large gaps the effect of the bending strain becomes important.

Consider, as an example, the problem extensively studied in [Genna and Gelfi 2012a], which has the following set of data: $L = 560$ mm; $E = 210000$ MPa; rectangular cross-section 5×50 mm; gap $s = 0.5$ mm; $\Delta = 11.2$ mm. If one adopts (3-2), one has immediately $\bar{\varepsilon} = 0.02$, and $F = 1050000$ N as the applied axial force; if one adopts the boundary condition in (3-1), one computes $\bar{\varepsilon} = 0.01978$ and $F = 1038600$ N. If one considers a gap $s = 1.0$ mm, then (3-1) yields $\bar{\varepsilon} = 0.01915$ and $F = 1005190$ N; but with $s = 5.0$ mm one finds $\bar{\varepsilon} = 0.009438$ and $F = 495491$ N, with a substantial difference between the two approaches. In this last case, the bending contribution to the axial displacement, given by the second term in (3-1), is $\Delta_b = 5.91476$ mm.

Similar results are obtained using a very different set of data, taken from the example studied in [Gelfi and Metelli 2007]: $L = 3000$ mm; $E = 210000$ MPa; rectangular cross-section 10×120 mm; gap $s = 1.0$ mm; $\Delta = 60.0$ mm. Using (3-2) one has $\bar{\varepsilon} = 0.02$ and $F = 5040000$ N; using (3-1) one finds $\bar{\varepsilon} = 0.01978$ and $F = 4983680$ N. Only with a gap $s = 10.0$ mm one finds a significant difference between the two approaches, (3-1) providing $\bar{\varepsilon} = 0.0094$ and $F = 2371250$ N.

Therefore, it seems reasonable to conclude that, if one restricts the attention to the case of small gaps and small buckled amplitudes, the use of (3-2) is perfectly adequate. In the presence of exceedingly large gaps a second-order approximation would lose validity altogether.

Some comments are now given about the important topic of the meaning of the obtained analytical results with reference to the calculation of the lateral thrust in actual BRBs. We still refer to a fully ideal BRB situation, in which linear elasticity holds for the core material, no friction exists between core and containment profiles, and the loading is monotonic.

Even in this ideal case, it seems impossible, in practice, to predict with accuracy the half-wavelength l_0. Owing to the effect of the imperfections, in fact, the actual configuration under any given value of the axial shortening Δ could be any of those herein considered, and the relevant value for ξ can take any of the values computed accordingly.

This fact could be confirmed numerically. The problem of [Genna and Gelfi 2012a] has been solved numerically several times using the FEM code ABAQUS [Hibbitt et al. 2013] using a mesh of 3000 Timoshenko linear beam elements, with frictionless unilateral contact against rigid surfaces in the case $k \to \infty$. Each analysis introduced a different type of initial imperfection, which was either a deviation from linearity of the beam axis or the presence of a small transversal load, in some case having a quick temporal variation in order to influence in a "random" way the formation of new buckled waves. Changing the type of this imperfection, for $\Delta = 11.2$ mm, i.e., $\bar{\varepsilon} = 0.02$, quite different solutions were predicted, with a number of waves variable from 1 to 3, with l_0 variable from 250 mm to 90 mm, and with a total lateral thrust variable from 17073 N to 103366 N.

Suggestions about a reasonable engineering compromise for the choice of parameter ξ will be given shortly.

Another difficult point concerns the calculation of the total thrust Q. Even though the unit thrust Q_i is not strongly dependent on the value of ξ in several cases (see for instance (3-54); but also in other

situations the unit thrust, for reasonable values of the parameters, does not depend too much on the value of ξ — see also Tables 1 and 2 on page 461), the value of the total thrust Q exhibits always a strong dependence on both ξ and, of course, L. The difficulty, here, derives from the adoption of (3-5) to relate the wave number to the wavelength: this expression furnishes real (as alternative to integer) values for N, which is not correct, since N has to be an integer.

This problem is of difficult solution as long as one needs to take into account also the stiffness k of the elastic connection spring. In this case, in fact, all the aspects of the solution become strongly coupled, and all the parameters of interest vary in a quite large range of values, depending on the actual value of k; the thrust can jump to infinity, which makes it completely unpredictable.

Nevertheless, considering that a correct estimate of the spring constant k is not so easy, and considering that the good functioning of a BRB depends anyway on a high stiffness of the containment structure, it can be safely concluded that an engineer should endeavor to design the containment profiles stiff enough to make them behave as almost rigid, i.e., in the range of values for k associated to the result $\xi \approx 1.4303$ for the pure PC situation for all the expected values of the axial force.

Then, by restricting the attention to the case $k \to \infty$, it is possible to reach some acceptable results. In the first place, the admissible values for ξ are now limited in the range $1.4303 \leq \xi \leq 4$. Considering that, in practice, asymmetric configurations will be more likely than fully symmetric ones, as also shown by experiments and numerical simulations (see for instance [Genna and Gelfi 2012a] and [Bregoli 2014]), one is lead to adopt values in the range $2.52875 \leq \xi \leq 3$, $\xi = 3$ being the simplest choice, not so far from the trivial average value $\xi = (1.4303 + 4)/2 = 2.72$.

One further reason for adopting the value $\xi = 3$ as an estimate for the wavelength derives from thinking in terms of elastic-plastic behavior, obviously important in engineering applications such as BRBs. In the elastic-plastic case, the axial force F can definitely reach and overcome the elastic limit for the compressed core. This means that at the contact points the bending moment contribution can not be high anyway, considering that the cross-section has almost fully exhausted its stress-carrying capacity because of the axial force alone. Therefore, one should reasonably expect a situation in which the bending moment is zero, or nearly so, at the contact points, which implies that coefficient ξ can assume the limit value $\xi_{\max} = 2$ for a PC situation, $\xi_{\max} = 3$ for an ALC situation, or $\xi_{\max} = 4$ for an SLC one. Considering that all these values are the maximum possible in each case, and that in a real situation (elastic-plastic, with friction, etc.) symmetry is less and less likely, it seems more appropriate to choose the asymmetric case value, i.e., $\xi = 3$.

Finally, recall also that values $\xi > 3$, with $k \to \infty$, correspond to situations in which two new waves would be formed simultaneously, a case that in reality does never occur; $\xi = 3$ seems therefore to be the highest possible value that can be reached in the case of an infinitely rigid connection spring, and a reasonable engineering choice, in the absence of information about imperfections.

According to this choice, the expression for the unit thrust to be adopted becomes (3-53), which, in the case of a rigid connection spring, reduces to (3-54).

Once agreed on this, then it is finally possible to tackle the problem of computing the total thrust on the basis of an integer number of waves.

If one attempts to make the TPE extreme with respect to feasible values of N, *with N an integer* (this can be easily done numerically), one finds results not much distant from the analytical ones given by the use of (3-5). It can be seen, actually, that, given ξ, the corresponding choice, for the correct integer N_{int},

is given by

$$N_{\text{int}} = \text{Int}(N + 0.5), \tag{4-1}$$

i.e., the nearest integer to N given by (3-5). Therefore, in computing the unit thrust Q for a given ξ, on the basis of (3-4), it is suggested to adopt expression (4-1) instead of (3-5).

In order to have an idea of the approximation provided by the proposed procedure, one can once more consider the two examples of [Genna and Gelfi 2012a] and [Gelfi and Metelli 2007]. Both geometries have been studied using the FEM code ABAQUS [Hibbitt et al. 2013], adopting a full 3D mesh for the core, with linear elasticity for the core material, and frictionless rigid surfaces for the containment. In the case of 3D analyses, the adopted imperfection was only a small fraction of the self weight of the beam, considered acting as a transversal load. In general, the FEM solutions obtained by means of continuum models tend to be less sensitive to imperfections than solutions given by beam models, and even less sensitive in the elastic-plastic range, as was also found in [Genna and Gelfi 2012a], and as will be discussed in work under way. The following numerical results have been obtained:

- geometry of [Genna and Gelfi 2012a] with $\Delta = 11.2$ mm; $l_0 \approx 70$ mm, $\xi \approx 2.06$; $N = 4$; $F = 938464$ N; $Q_i = 24438$ N; $Q = 97750$ N;

- geometry of [Gelfi and Metelli 2007] with $\Delta = 60.0$ mm; $l_0 \approx 150$ mm, $\xi \approx 2.44$; $N = 9$; $F = 5466330$ N; $Q_i = 143060$ N; $Q = 1287540$ N.

The corresponding analytical results, for $k \to \infty$, are shown in Tables 1 and 2, respectively, where all the possible choices of parameters ξ and β have been considered, in order to show the relevant differences.

ξ	β	l_0 [mm]	N_{int}	Q_i [N]	Q [N]
1.4303	0.5	45.86	6	29447	176682
2	0.5	64.13	4	32747	130989
2.52875	0.3023	81.08	4	31037	124148
3	0.3333	96.2	3	32747	98242
3.58639	0.2212	114.99	2	31641	63282
4	0.25	128.26	2	32747	65495

Table 1. Analytical results for the example of [Genna and Gelfi 2012b] with $k \to \infty$. $\Delta = 11.2$ mm; $F = 1050000$ N.

ξ	β	l_0 [mm]	N_{int}	Q_i [N]	Q [N]
1.4303	0.5	91.72	16	141345	2261514
2	0.5	128.26	12	157187	1886244
2.52875	0.3023	162.16	9	148978	1340798
3	0.3333	192.4	8	157187	1257495
3.58639	0.2212	229.99	7	151878	1063143
4	0.25	265.51	6	157187	943122

Table 2. Analytical results for the example of [Gelfi and Metelli 2007] with $k \to \infty$. $\Delta = 60$ mm; $F = 5040000$ N.

It is apparent that the total thrust Q takes values in a quite large range, even though the unit thrust Q_i does not depend much on the considered configuration. Adopting the proposed values for ξ and β ($\xi = 3$, $\beta = 1/\xi = 0.3333$), the error on the most interesting quantity, i.e., the total lateral thrust Q, is of the order of 0.02 in the worst case, which appears satisfactory, under the circumstances.

5. Conclusions

New calculations have been developed for the problem of the buckling of an elastic compressed beam restrained by unilateral frictionless contact against rigid surfaces that can translate elastically with respect to each other. Special attention has been devoted to devising a technique for obtaining directly the wave number and the associated thrust produced by the beam, when in contact against the rigid surfaces, for a prescribed value of the axial shortening. Even though some analytical results could be obtained, it appears that a precise calculation of the current number of buckled waves, and thus of the total lateral thrust, is impossible. Several alternative configurations can in principle occur under the same axial load, and the one actually followed depends on the existing imperfections, which can not be defined with precision.

With reference to the design of BRBs, the calculations developed herein lead to conclude that a good engineering choice is to enforce as strongly as possible a rigid constraint between the rigid surfaces, and that, also in view of the likely preference of buckled shapes for nonsymmetric configurations, a good choice for the coefficient ξ of the equation (3-11) governing the wavelength should be $\xi = 3$. The comparison with some numerical simulations has shown that, in this way, reasonably accurate results can be found under the assumptions of validity of the theory herein developed.

It is worth remarking that the choice $\xi = 3$ provides a relationship, between axial force and buckled wavelength, that implies an axial force 9 times larger than the one given by Euler's formula (see (3-12)), which is obviously not applicable in this situation.

The obtained results should constitute a starting point for the engineering design of BRBs, although the real situation, with BRBs, includes plastic deformations, contact with friction, and cyclic loading. Further work, based on the results herein presented, will tackle these more general aspects.

Acknowledgements

References

[Alart and Pagano 2002] P. Alart and S. Pagano, "Confined buckling of inextensible rods by convex difference algorithm", *C. R. Mécanique* **330**:12 (2002), 819–824.

[Bregoli 2014] G. Bregoli, *Studio di dispositivi in acciaio per il miglioramento sismico di edifici in c. a.*, Ph.D. Thesis, Dept. Civil Engineering, University of Brescia, 2014.

[Chai 1998] H. Chai, "The post-buckling response of a bi-laterally constrained column", *J. Mech. Phys. Solids* **46**:7 (1998), 1155–1181.

[Chai 2001] H. Chai, "Contact buckling and postbuckling of thin rectangular plates", *J. Mech. Phys. Solids* **49**:2 (2001), 209–230.

[Chai 2002] H. Chai, "On the post-buckling behavior of bilaterally constrained plates", *Int. J. Solids Struct.* **39**:11 (2002), 2911–2926.

[Domokos et al. 1997] G. Domokos, P. Holmes, and B. Royce, "Constrained Euler buckling", *J. Nonlinear Sci.* **7**:3 (1997), 281–314.

[Gelfi and Metelli 2007] P. Gelfi and G. Metelli, "Prova sperimentale di un elemento diagonale di controvento ad instabilità controllata", in *Proceedings, XXI Congresso C.T.A.: Costruire con l'acciaio*, 1–3 October 2007, Catania, Italy, 169–176 (2007).

[Genna and Gelfi 2012a] F. Genna and P. Gelfi, "Analysis of the lateral thrust in bolted steel buckling-restrained braces, 1: Experimental and numerical results", *J. Struct. Eng.* (*ASCE*) **138**:10 (2012), 1231–1243.

[Genna and Gelfi 2012b] F. Genna and P. Gelfi, "Analysis of the lateral thrust in bolted steel buckling-restrained braces, 2: Engineering analytical estimates", *J. Struct. Eng.* (*ASCE*) **138**:10 (2012), 1244–1254.

[Hibbitt et al. 2013] D. Hibbitt, B. Karlsson, and P. Sorensen, *ABAQUS user's manuals*, Release 6.13, Dassault Systèmes/Simulia, Providence, RI, 2013, http://50.16.176.52/v6.13.

[Holmes et al. 1999] P. Holmes, G. Domokos, J. Schmitt, and I. Szeberényi, "Constrained Euler buckling: an interplay of computation and analysis", *Comput. Methods Appl. Mech. Eng.* **170**:3-4 (1999), 175–207.

[Muradova and Stavroulakis 2007] A. D. Muradova and G. E. Stavroulakis, "A unilateral contact model with buckling in von Kármán plates", *Nonlinear Anal. Real World Appl.* **8**:4 (2007), 1261–1271.

[Pocheau and Roman 2004] A. Pocheau and B. Roman, "Uniqueness of solutions for constrained Elastica", *Physica D* **192**:3-4 (2004), 161–186.

[Roman and Pocheau 2002] B. Roman and A. Pocheau, "Postbuckling of bilaterally constrained rectangular thin plates", *J. Mech. Phys. Solids* **50**:11 (2002), 2379–2401.

[Tzaros and Mistakidis 2011] K. A. Tzaros and E. S. Mistakidis, "The unilateral contact buckling problem of continuous beams in the presence of initial geometric imperfections: an analytical approach based on the theory of elastic stability", *Int. J. Non-Linear Mech.* **46**:9 (2011), 1265–1274.

[Villaggio 1979] P. Villaggio, "Buckling under unilateral constraints", *Int. J. Solids Struct.* **15**:3 (1979), 193–201.

FRANCESCO GENNA: francesco.genna@unibs.it
Department of Civil Engineering, University of Brescia, Via Branze, 43, I-25123 Brescia, Italy

GUIDO BREGOLI: g.bregoli@unibs.it
Department of Civil Engineering, University of Brescia, Via Branze, 43, I-25123 Brescia, Italy

JOURNAL OF MECHANICS OF MATERIALS AND STRUCTURES